DOI: 10.1002/chem.200500292

Light-Induced Transformation of Alkylurea Derivatives in Aqueous TiO_2 Dispersion

Paola Calza,*[a] Claudio Medana,[a] Claudio Baiocchi,[a] Hisao Hidaka,[b] and Ezio Pelizzetti[a]

Abstract: The light-induced degradation of alkylurea derivatives under simulated solar irradiation has been investigated in aqueous solutions containing TiO_2 as a photocatalyst. Herein, we will focus on how the presence of one or more methyl (or ethyl) groups on urea modifies the kinetics of disappearance and influences both the ratio and the extent of the inorganic nitrogen formation caused by different degradation pathways. In the present work, we have elucidated a mechanism for the formation of transformation products of the alkyl derivatives by combining several analytical and spectroscopic procedures and the theoretical simulation of ab initio calculations. In all cases, N-demethylation represents only a secondary pathway, while the main transformation proceeds through an unexpected cyclization, involving (m)ethyl- and di(m)ethylureas with the formation of (methyl)amino-2,3-dihydro-1,2,4-oxadiazol-3-one as the principal intermediate of the reaction (with a yield of 60%). This behaviour is rather unexpected and in contrast with the typical photocatalyzed transformation pathways, which proceed through the formation of more simple structures.

Keywords: alkylureas · cyclization · nitrogen · photocatalysis · titanium

Introduction

The understanding of all possible processes involved in the natural evolution of nitrogen-containing compounds is extremely important, not only because nitrogen constitutes a key element of nutrient cycles, but also because a large number of anthropogenic compounds encloses one or more nitrogen atoms. Although the patterns of transformation on macromolecules containing nitrogen have been widely investigated, at present limited attention has been paid to small molecules, especially those containing amino groups. Their transformation products have not yet been identified, mainly due to the analytical complexity involved with their determination (i.e., small molecules often being very hydrophilic). These structures represent the missing link in the transformation of organic into inorganic species. We have investigated the classes of urea, guanidine, thiourea, and their derivatives. These structures are building blocks of proteins, DNA, pesticides, drugs, and other biomolecules, and the understanding of their transformation pathways is relevant to several areas of research. Herein, we will focus on urea and alkylurea derivatives only, while the above-mentioned compounds will be discussed in forthcoming works. A complete characterization of the intermediates has been obtained by HPLC/MS analysis, followed by NMR and IR investigations and supported by ab initio calculations, thus allowing the definition of a transformation mechanism applicable to methyl- and ethylurea derivatives.

Urea and alkylureas are building blocks for several anthropogenic compounds, such as pesticides and fertilizers,[1,2] natural compounds like caffeine,[3] constituents of drugs, antiepileptic and HIV drugs,[4,5] and transformation products of DNA.[6] In addition, they have been identified as final products of natural degradation.[7] The synthesis of urea represents the first synthetic pathway identified in organic chemistry.[8] Similarly, the same synthetic reaction has been obtained by adopting the photocatalytic process with TiO_2 as the photocatalyst.[9] For this reason, we have employed a light-induced process with TiO_2 to produce the transformation products of urea derivatives. It is worth noting that heterogeneous photocatalysis with irradiated semiconductors involving oxido-reductive reactions has been established as an effective analytical method, not only for degradation and

[a] Dr. P. Calza, Prof. C. Medana, Prof. C. Baiocchi, Prof. E. Pelizzetti
Dipartimento di Chimica Analitica, Università di Torino
Via P. Giuria 5, 10125 Torino (Italy)
Fax: (+39) 011-670-7615
E-mail: paola.calza@unito.it

[b] Prof. H. Hidaka
Meisei University
Frontier Research Center for the Environmental Science
2–1–1- Hodokubo, Hino, Tokyo 191–8506 (Japan)

final mineralization of several organic compounds,[10–13] but also for acquiring information on naturally occurring transformations. Specific examples of the applicability of this method are represented by reactions occurring in the environment[14,15] and in living organisms.[16,17] In both cases, some of the intermediates identified through a photocatalytic process have been found in soil samples[14,15] and in the animal liver.[16,17] Nevertheless, despite its extensive applications, several mechanistic aspects are still unexplained. One of the open issues is represented by the fate of bound nitrogen, for which the transformation into inorganic ions (i.e., ammonium and nitrate) has been observed but the detailed mechanism of their formation has not been elucidated to date. This is caused by the complexities associated with the identification of the final organic products in the photocatalytic degradation of materials containing nitrogen.

To investigate the fate of the intermediates, bound nitrogen and organic carbon mineralization, we have evaluated the role of electron donor groups on the amino subtituents in the present work. The existence of atypical differences in the formation of intermediates has prompted us to verify if these peculiarities are also maintained in a homogeneous system. We have therefore performed experiments employing H_2O_2 as a reactant.

Experimental Section

Materials and photochemical apparatus: Urea (U), methylurea (MU), 1,1′-dimethylurea (1,1′-DMU), 1,3-dimethylurea (1,3-DMU), tetramethylurea (TMU), ethylurea (EU), 1,1′-diethylurea (1,1′-DEU), and 1,3′-diethylurea (1,3′-DEU) were all purchased from Aldrich and were used as received. Ammonium chloride (Carlo Erba), potassium nitrate (Merck) and sodium nitrite (Carlo Erba) were used after drying. HPLC grade water was obtained from MilliQ System Academic (Waters, Millipore). HPLC grade methanol (BDH) was filtered through a 0.45 μm filter before use. Ammonium acetate (reagent grade) was purchased from Fluka.

Prior to analysis the TiO_2 powder (Degussa P25 photocatalyst) was pretreated to avoid possible interference from ions adsorbed on the photocatalyst. The powder was irradiated and washed with distilled water until no signal caused by chloride, sulphate or sodium ions could be detected by ion chromatography.

The irradiations were performed in air-saturated cells using a 1500 W xenon lamp (Solarbox, CO.FO.MEGRA, Milan, Italy) with a 340 nm cut-off filter, simulating AM1 solar light. The total photon flux (340–400 nm) in the cell and the temperature during irradiation were kept constant for all experiments, that is, at 1.35×10^{-5} einstein min^{-1} and 50 °C, respectively. The irradiation was carried out in a suspension of alkylurea (15 mg L^{-1}) and TiO_2 (200 mg L^{-1}) in water (5 mL). The entire content of the cells was filtered through a 0.45 μm filter and then analyzed by an appropriate technique.

When using H_2O_2 (1×10^{-2} M) as a reactant, all of the settings were maintained, except for using a Philips UV lamp as a irradiation system.

Analysis of photochemical products: The chromatographic separations were run on a C18 column Phenomenex Luna, 150×2.0 mm (Phenomenex, Torrance, CA, USA). Injection volume was 20 μL with a flow rate of 0.2 mL min^{-1}. A gradient mobile phase was adopted: 5:95 to 40:60 in 25 min with 5 mM pH 6.8 of a methanol/aqueous ammonium acetate mixture. A LCQ Deca XP PLUS ion trap mass spectrometer (Thermo) equipped with an atmospheric pressure interface and an ESI ion source was used. The LC column effluent was delivered into the ion source by using nitrogen as sheath and auxiliary gas (Claind Nitrogen Generator apparatus). The needle voltage was set at 4.5 kV. The heated capillary value was maintained at 250 °C. The acquisition method used was previously optimized in the tuning sections for the parent compound in order to achieve maximum sensitivity (capillary, magnetic lenses, and collimating octapoles voltages).

A Dionex instrument with a conductimeter detector was employed. The determination of ammonium ions was performed by adopting a CS12A column and 25 mM methanesulfonic acid as the eluant with a flow rate of 1 mL min^{-1}. Under such conditions, the retention time was 3.9 min. The anions were analysed by using a AS9HC anionic column and a mixture of $NaHCO_3$ (12 mM) and K_2CO_3 (5 mM) at a flow rate of 1 mL min^{-1}. Under such experimental conditions the retention times were 4.20, 6.63, and 9.58 min for formic acid, nitrite, and nitrate, respectively.

Total organic carbon (TOC) was measured on filtered suspensions using a Shimadzu TOC-5000 analyzer (catalytic oxidation on Pt at 680 °C). Calibration was achieved by injecting standards of potassium phthalate.

The main intermediate formed from MU was characterized as follows. MU (400 mL, at the concentration of 300 mg L^{-1}) was irradiated and the cell content eluted on a C18 column with a flow rate of 8 mL min^{-1}. The fractions corresponding to the peaks observed by the HPLC/UV analysis were collected and lyophilized (in a Bruker lyophilizer). NMR and IR measurements as well as TOC analysis were performed on the obtained powder in order to verify the correspondence with the structure hypothesized. ^{1}H NMR (200 MHz, D_2O, 25 °C, TMS): $\delta=8.7$ (s), 8.2 ppm (s); ^{13}C NMR: $\delta=166.20$, 164.37 ppm; IR: $\nu=1107$, 1209 (C–N), 1675 (C=O), 1398 cm^{-1} (cycle); ESI-MS: m/z (%): 102 (100) $[M+H]^+$.

Computer simulations: Molecular orbital simulation of frontier electron densities and point charges of all atoms for urea and formamide was done by using the MOPAC/AM1 wavefunction. The computer simulations were carried out using the Gaussian 98 system (IBM-RS6000-G98Rev; B3LYP/6–31G). A geometrical configuration was determined by preoptimized calculation of the mechanics by using augmented MM3, followed by geometrically optimized calculations in MOPAC using AM1 parameters. Solvation effects in water were simulated by using COSMO (also available in the CAChe package).

Results and Discussion

In a previous investigation on the photocatalytic degradation of formamide and urea in the presence of titanium dioxide,[18] specific differences were identified. While formamide was easily degraded ($t_{1/2}$ 0.2 h), urea was slowly decomposed ($t_{1/2}$ 5 h). Moreover, the fate of the bound nitrogen displayed a different behaviour; both the rate and the ratio of the NH_4^+ and NO_3^- ion evolution varied (the ratio $[NH_4^+]/[NO_3^-]$ changed from 2:1 to 1:2 for formamide and urea, respectively). Given that the nitrogen oxidation state is −3 in both cases, the remarkable differences in the degradation rate and in the final nature of the nitrogen atoms (both originating from an amido group) can be rationalized by considering the carbon oxidation state or, alternatively, the presence/absence of extractable hydrogen. This prompted us to investigate how the presence of alkyl groups on the amino moiety may influence the kinetics and the mechanism of transformation of the urea derivatives.

The basic principles of photocatalysis have been extensively discussed elsewhere[10–13] and will only be briefly presented here. The primary photochemical event, following the near-UV light absorption by TiO_2 ($\lambda<$ 380 nm), is the generation of electron/hole pairs in the bulk of the semicon-

Table 1. Rate of disappearance of the methyl- and ethylurea derivatives in the presence of TiO_2 (200 mg L^{-1}) or H_2O_2 (5×10^{-3} M).

	Methylurea	1,1′-Dimethylurea	1,3′-Dimethylurea	Tetramethylurea	Ethylurea	1,1′-Diethylurea	1,3′-Diethylurea
TiO_2, rate [h^{-1}]	10.33	11.71	12.52	8.87	9.77	8.92	10.32
H_2O_2, rate [h^{-1}]	25.63	–	21.38	26.15	–	–	–

ductor. The charge carriers can either recombine or migrate to the surface where they are ultimately trapped. Electrons are trapped as Ti^{III} and the holes as radical hydroxyl groups. If electron-acceptor or electron-donor groups are present at the surface, interfacial electron transfer may also occur. The organic substrate reacts with formed active species (oxidants or reductants) depending on its initial oxidation state, the nature of substituents forming radicals and other species that are further oxidized or reduced.

Table 1 summarizes the rate of disappearance of alkylurea derivatives in the presence of TiO_2 or H_2O_2. Both the methyl- and ethylurea derivatives have shown to follow a first-order kinetic rate of decay. The disappearance of the initial compounds is easily achieved by all structures. What is rather surprising is the variable formation of intermediate products, as we will discuss hereafter.

Methylurea derivatives

N-methylurea: The key intermediate product formed by the photoinduced transformation of MU with TiO_2 has been observed with HPLC-DAD at $t_R = 2.40$ min; this transformation occurs within a few minutes and reveals a strong absorption in the UV, but no signal is found with MS analysis (neither positive nor negative ions). The latter entailed further work in the compounds isolation, characterization and quantification as described in the Experimental Section.

The structure of the unknown compound was confirmed to be 5-amino-2,3-dihydro-1,2,4-oxadiazol-3-one (AO) on the basis of ^{13}C and ^{1}H NMR signals and IR spectrum. The existence of the tautomeric structures, as shown in Scheme 1,[19] accounts for the signal observed in the ^{1}H NMR spectrum. It can exist as either a lactim or lactam form, so justifying that only two peaks appear in the ratio 2:1. This assumption is confirmed by the IR spectral analysis. Further evidence derives from a direct injection into the mass spectrometer of the isolated (and concentrated) compound, showing a weak signal at $[M+H]^+$ 102, and from the C/N ratio evaluated through the TOC and CI measurements. Finally, the compound was synthesized by following the procedure as found in references [19,20]. It has the same retention time and spectra of the species found during MU degradation. Taken together, such data allow the quantification of the unknown compound formed from MU.

The intermediate compounds deriving from MU degradation as a function of the irradiation time are depicted in Figure 1. This suggests that the pathway leading to AO is the most important one, accounting for almost 60% of the initial compound transformation. The N-demethylation reaction also occurs, although to a considerably lesser extent. The detachment of a methyl group from the parent molecule leads to methanol and, through a sequence of oxidative attacks, to the formation of formic acid.[21] The possible transformation pathways followed by alkylurea derivatives are postulated in Scheme 2, while acronyms and molecular weights of studied compounds are reported in Table 2. A closer inspection on MU transformation pathways reveals that while the first one leads to AO (labelled **1** in Scheme 2), other routes can lead to urea (**2**, formed at 1.33×10^{-5} M) and *N*-methylformamide (MF, **3**). These last structures can be successively transformed into formamide (**4**).

Although identical intermediates have been detected both with TiO_2 and H_2O_2, some differences were identified in their distribution. In the experiments performed with H_2O_2 the formation of AO is reduced by a diverse radical formation, while the yield of urea is enhanced (6.67×10^{-5} M).

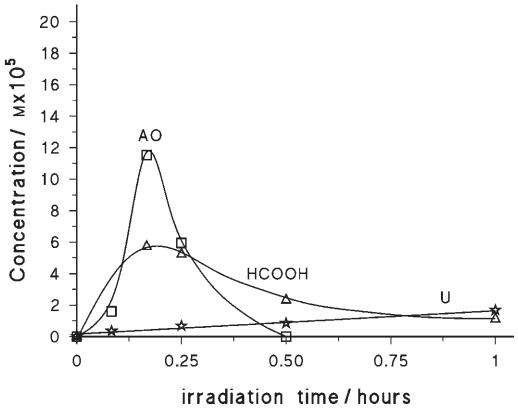

Figure 1. Degradation of MU (2×10^{-4} M) on TiO_2 and the formation of the intermediate compounds.

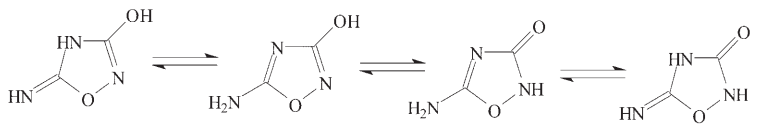

Scheme 1. Tautomeric forms of the key intermediates during MU degradation. ^{1}H NMR (200 MHz, D_2O): $\delta = 8.2$ and 8.7 ppm, ^{13}C NMR: $\delta = 164.20$ and 166.20 ppm.

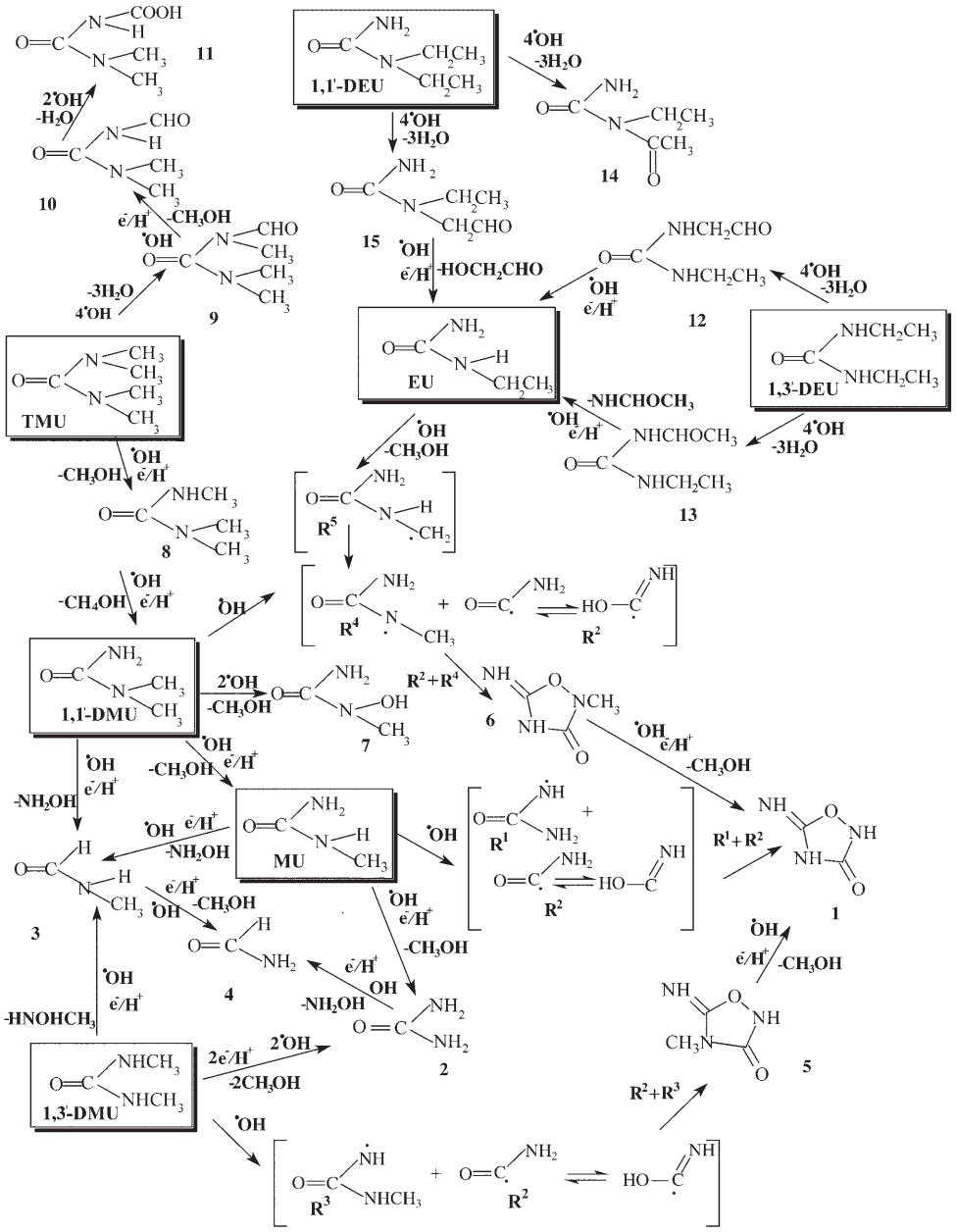

Scheme 2. Photocatalytic transformation pathways followed by methyl- and ethylurea derivatives. For schematic purposes, in all the reactions the oxidant species is indicated as a ·OH radical. However, the oxidant species formed during TiO_2 illumination includes $\cdot OH_{ads}$, $\cdot OH_{aq}$, and H^+.[11]

Dimethylureas: The degradative process involving 1,3-DMU or 1,1′-DMU gives rise to the formation of the species shown in Figure 2A and B, respectively. Several analogies with MU were identified by HPLC analysis showing peaks at t_R 3.67 min for 1,1′-DMU and at t_R 4.01 min for 1,3-DMU. Both peaks are characterized by a strong UV adsorption, but no signal was observed in the MS data (neither positive nor negative ions). Based on the described MU and their retention times, it is reasonable to assume that a structure similar to the one identified from MU degradation is formed. This structure is characterized by a methyl group, located in different positions on the heteroring, in lieu of a hydrogen atom. Therefore, the formation of 4-methyl-5-amino-2,3-dihydro-1,2,4-oxadiazol-3-one (4-MAO, labelled **5** in Scheme 2) and 2-methyl-5-amino-2,3-dihydro-1,2,4-oxadiazol-3-one (2-MAO, **6**) from 1,3-DMU and 1,1′-DMU, respectively, is proposed (see Scheme 2). These structures are easily degraded yielding AO, as proposed in Scheme 2. Hence, the formation of a cyclic compound represents the key degradation pathway.

The formation of AO from methyl derivatives is accomplished by the detachment of the methyl group and the formic acid formation. Minor competitive degradation pathways occur, leading to a demethylation process. The formation of methylurea, hydroxylmethylurea (**7**), and methylformamide (**8**) is observed from 1,3-DMU. Urea is finally

Table 2. Summary of the acronyms used for the identified structures.

Name	No.	Acronym	M_r
methylurea	–	MU	74
1,1′-(1,3′)-dimethylurea	–	1,1′-(1,3′)-DMU	88
tetramethylurea	–	TMU	116
ethylurea	–	EU	88
1,1′-(1,3′)-diethylurea	–	1,1′-(1,3′)-DEU	116
5-amino-2,3-dihydro-1,2,4-oxadiazol-3-one	**1**	AO	101
urea	**2**	U	60
methylformamide	**3**	MF	59
formamide	**4**	–	45
4-methyl-5-amino-2,3-dihydro-1,2,4-oxadiazol-3-one	**5**	4-MAO	115
2-methyl-5-amino-2,3-dihydro-1,2,4-oxadiazol-3-one	**6**	2-MAO	115
hydroxylmethylurea	**7**	–	90
trimethylurea	**8**	tri-MU	102
N-formyltrimethylurea	**9**	ATri-MU	130
N-formyldimethylurea	**10**	ADMU	116
N-carboxydimethylurea acid	**11**	AADMU	132
N-ethyl-*N*′-formylmethylenurea	**12**	–	130
N-ethyl-*N*′-formyl-*N*′-methylurea	**13**	–	130
N-ethyl-*N*-acetylurea	**14**	–	130
N-ethyl-*N*-formylmethylenurea	**15**	–	130

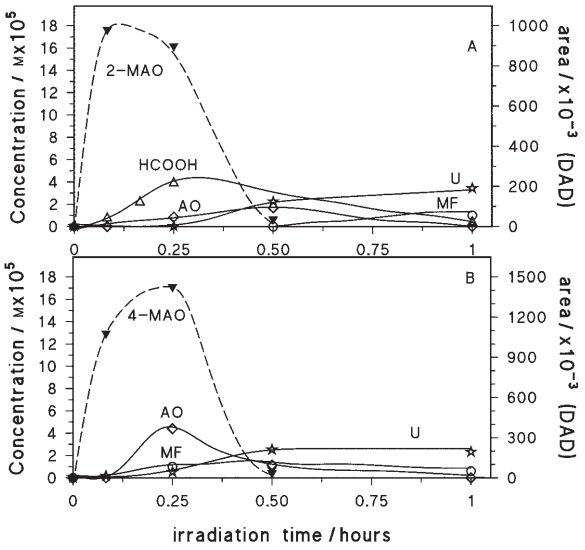

Figure 2. Degradation of DMU (1.68×10^{-4} M) on TiO_2 and the formation of the intermediate compounds from A) 1,3-DMU and B) 1,1′-DMU; open symbols and continuous lines refer to the left *y* axis, while solid symbols and dotted lines refer to the right *y* axis.

formed from 1,1′- and 1,3-DMU, at a yield of approximately 3.33×10^{-5} M, both with TiO_2 and H_2O_2. The same category of intermediates is formed when employing H_2O_2.

Tetramethylurea: The intermediates profiles of TMU as a function of the irradiation time are depicted in Figure 3. A demethylation process occurs with the subsequent formation of trimethylurea (tri-MU, **8**), 1,1′-DMU and urea. Initially, a small quantity of MU is also observed that is quickly transformed into urea (with a yield of 3.33×10^{-5} M). Therefore, the role of the demethylation process is similar with both DMU and TMU derivatives. At the same time traces of 2-MAO are detected, which emphasizes the occurrence of the same degradation pathways as already described above.

Nevertheless, in contrast with MU and DMU derivatives, the cyclization reaction represents only a minor pathway. Concurrent to the progression of the demethylation, degradation through oxidation of the methyl groups occurs. Several species have been identified through HPLC/MS^n, the characteristic MS and MS^2 losses of which are summarized in Table 2. It leads to the formation of a species at $[M+H]^+$ 131, recognized as *N*-formyltrimethylurea (ATri-MU, **9** in Scheme 2), suddenly transformed into *N*-formyldimethylurea (ADMU, **10** $[M+H]^+$ 117) and afterwards into *N*-carboxydimethylurea acid (AADMU, **11** $[M-H]^-$ 130).

Fate of the nitrogen: The fate of nitrogen in different MU derivatives is shown in Figure 4. Nitrogen-containing moieties in organic compounds can be transformed photocatalytically into either N_2, NH_3/NH_4^+, and/or nitrite and nitrate ions, the ratio depending on the different features of the N-containing structure.[22,23] Moreover, the relative amount of ammonium and nitrate formation is related to the initial transformation mechanism. The final fate of organic nitrogen in photocatalytic processes has been reported to be essentially related to the initial oxidation state of nitrogen in the organic compounds,[24,25] the presence/absence of oxygen and, in few cases, the structure of the organic compound

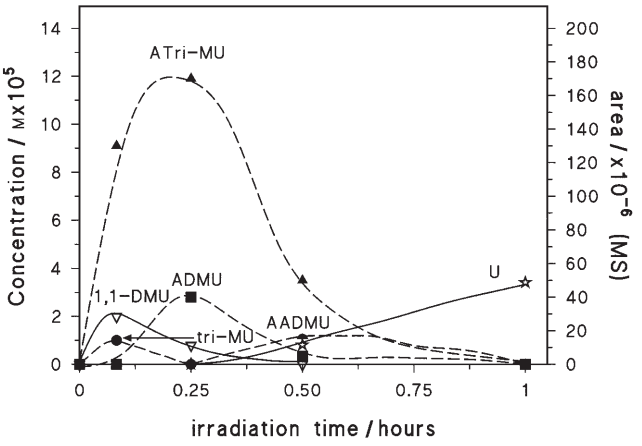

Figure 3. Degradation of TMU (1.29×10^{-4} M) on TiO_2 and the formation of intermediate compounds. Open symbols and continuous lines refer to the left *y* axis, while solid symbols and dotted lines refer to the right *y* axis.

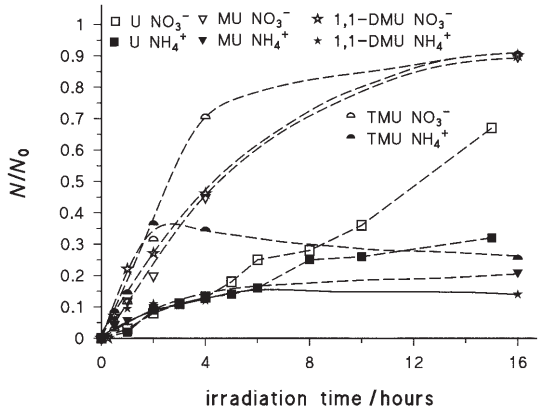

Figure 4. Comparison of the nitrogen evolution in urea (U) and MU derivatives.

(e.g., 4-nitrosophenol vs nitrosobenzene).[26,27] Nevertheless, the fate of nitrogen initially linked as an amido group is reported to show different ratios of $[NH_4^+]/[NO_3^-]$ for formamide with respect to urea under photocatalytic conditions. Hence, an interesting correlation between the carbon oxidation state and the final fate of bound nitrogen is observed. It seems that the fate of the nitrogen atoms (−3 oxidation state in both compounds) is governed by the initial oxidation state of carbon (+4 in urea and +2 in formamide).[18]

Given that the transformation of ammonium into nitrate is negligible,[28] ammonium ions are formed directly from the release of nitrogen as ammonia, with an oxidation state of −3 of the bound nitrogen. In contrast, nitrate formation can be achieved either through the release of a nitro group, with formation of nitrite ions (which are further oxidized to nitrates) or through a sequence of oxidative steps from hydroxylamine.

In light of the above, it is relevant to compare the fate of nitrogen observed with the MU with respect to unsubstituted urea. In the case of urea (further to the formation of nitrate) 30% of the nitrogen is converted into ammonium ions. This accounts for the ratio $[NH_4^+]/[NO_3^-]$ observed with urea (30:65 ≈1:2).[18] The given ratio suggests an ·OH attack on the carbon atom, after the (slow) attack on the N atom, probably leading to the formation of carbamic acid. Carbamic acid could then support both an oxidative and reductive sequence on the carbon atom. After the detachment of the first amino group and by assuming that carbamic acid is a key intermediate, the second amino group should follow the same fate of formamide. This would imply that a second N atom would form approximately 30% of ammonium and 15% of nitrate of the stoichiometric amount (2:1 ratio on 50%). The first amino group gives a nitrate formation in stoichiometric amounts, that is, 50% of the organic nitrogen conversion, leading to 65% overall nitrate ion formation.

Although in all of the MUs considered the nitrogen is preferentially released as nitrate ions, it occurs at different ratios and rates of mineralization. After 16 h of irradiation the mineralization is completed in all cases. The rate of the mineralization increases with the number of methyl groups. Mineralization of TMU is already completed after 4 h of irradiation. When comparing urea and *N*-methylurea, after 16 h of irradiation (complete mineralization is achieved), the ratio $[NO_3^-]/[NH_4^+]$ changes from 1:2 to 1:4 for U and MU, respectively. The higher percentage in nitrate formation becomes already apparent in the initial part of the process. In fact, after 4 h of irradiation the formation of 10% of ammonium is achieved for both structures, while nitrate formation is enhanced for MU; 40% of ammonium instead of 10% is formed. This indicates that the process leading to demethylation contributes to the mineralization and formation of ammonium ions to a lesser extent, while the part of the process that proceed through the AO formation allows mineralization and favours the oxidation of nitrogen contained in the structure.

For the DMUs, the ratio $[NO_3^-]/[NH_4^+]$ is significantly influenced by the location of the methyl groups. For 1,1′-DMU both methyl groups are located on the same nitrogen atom, whereby the oxidation of the nitrogen is strongly favored (ratio 6:1). For 1,3-DMU, two methyl groups are located on two different amino groups (ratio 2:1) and the same considerations as for MU can be taken. This difference agrees with the reduced demethylation process observed in the case of 1,1′-DMU, while the existence of a similar rate of mineralization matches the considerations described above, as well as the occurrence of the same transformation mechanism of the two structures.

In the case of TMU, nitrate formation is favored and easily achieved. In fact, after 4 h of irradiation organic nitrogen is completely transformed into inorganic ions, mainly as nitrate (80%). The high concentration of nitrate ions could be caused by the release of *N*-hydroxycarbamic acid, with the corresponding formation of a cyanate derivative. In fact, the cyanate group releases the nitrogen as nitrate ions, as previously reported.[29]

Carbon mineralization: The final transformation of organic carbon into carbon dioxide occurs in all of the investigated molecules at the same rate observed as for the nitrogen release. Moreover, complete mineralization is achieved for all alkyl derivatives within 24 h of irradiation, while in the case of urea up to 50 h of irradiation are needed.[18]

Ethylurea derivatives: The unusual differences observed with the fate of nitrogen and the evolution of the intermediates deriving from the substitution of hydrogen atoms by methyl groups have prompted us to check if this behaviour is still maintained when the substituents are ethyl instead of methyl groups. We have investigated ethylurea (EU), 1,1′-diethylurea (1,1′-DEU), and 1,3′-diethylurea (1,3′-DEU).

Ethylurea: Figure 5A illustrates the TOC disappearance and the fate of nitrogen for EU, while the intermediates profiles are reported in Figure 5B. Looking closer at the evolution of the intermediates, the formation of the key species evidenced during 1,1′-DMU degradation, that is, 2-MAO, is observed. Its formation passes through the generation of the

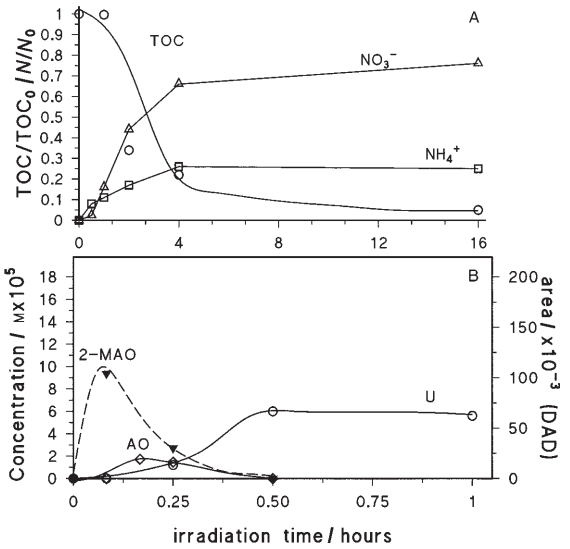

Figure 5. Degradation of EU (1.68×10^{-4} M) on TiO_2; A) disappearance of TOC and the formation of nitrate and ammonium, B) evolution of the intermediate compounds. Open symbols and continuous lines refer to the left *y* axis, while solid symbols and dotted lines refer to the right *y* axis.

radicals R^2 and R^5 (Scheme 2). The transposition of a hydrogen atom on the latter radical leads to the formation of R^4, the key radical for the 2-MAO formation. It is the only species evidenced at short irradiation times, rapidly being converted into AO by the mechanism described above. The successive formation of urea is also observed at a yield of 5×10^{-5} M.

Complete mineralization is achieved after 16 h of irradiation. At the same time, nitrogen is released in stoichiometric amount, with a ratio $[NO_3^-]/[NH_4^+]$ of 3:1. This strongly resembles the fate followed by 1,3-DMU, underlying the close relationship existing between the mechanism of transformation of these two structures.

Diethylureas: Interestingly, despite similar rates in nitrogen and carbon mineralization, different distributions of nitrate and ammonium ions were observed in comparison with previously described compounds. In both cases ammonium is initially formed in a noticeable amount. Only with longer irradiation times (50 h) is a strong predominance of nitrate formation observed. This is shown in Figure 6a, in which the TOC and nitrogen release profiles for 1,1′- and 1,3-DEU are reported.

Figure 6B and C show the intermediates distribution for 1,3′- and 1,1′-DEU. Two structures with the same *m*/*z* ratio (*m*/*z* 131) are initially formed for both derivatives, which can be ascribed to the oxidation of a methyl group into a keto group. The existence of more than one derivative along with the same *m*/*z* ratio is caused by the nonselectivity of ·OH radical attacks. In agreement with the retention times observed and their MS^2 peculiar losses (see Table 3), we have concluded that the structures *N*-ethyl-*N*′-formylmethylenurea (**12** in Scheme 2) and *N*-ethyl-*N*′-formyl-*N*′-methylurea (**13**) for 1,3′-DEU and *N*-ethyl-*N*-acetylurea (**14**) and

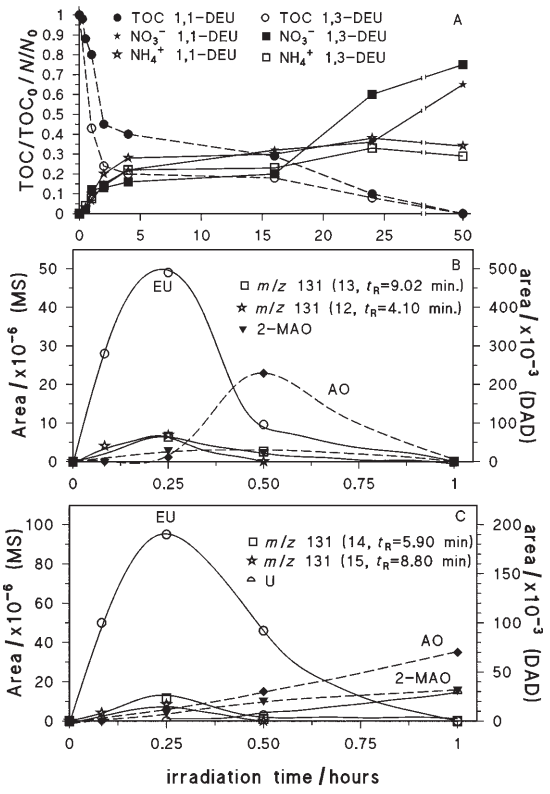

Figure 6. Degradation of DEUs (1.29×10^{-4} M) on TiO_2. A) Disappearance of TOC and the formation of nitrate and ammonium, 1,1′-DEU and 1,3′-DEU. B and C) Formation of intermediate compounds from 1,3′-DEU and 1,1′-DEU, respectively. Open symbols and continuous lines refer to the left *y* axis, while solid symbols and dotted lines refer to the right *y* axis.

Table 3. Main fragments coming from MS^2 spectra of some species shown in Scheme 2. The relative frequencies are reported in brackets.

$[M+H]^+$	No.	MS^2 fragments	Associated losses
131	**9**	72(100)	CHO–$NHCH_3$
117	**10**	72(100)	CHO–NH_2
131	**12**	60(100)	C_2H_5–N=C=O
131	**13**	60(100)	C_2H_5–N=C=O
131	**14**	60(65)	C_2H_5–N=C=O
		88(100)	HN=C=O
131	**15**	113(100)	H_2O
		60(57)	C_2H_5–N=C=O

N-ethyl-*N*-formylmethylenurea (**15**) for 1,1′-DEU are formed.

Additional analysis of 1,3′-DEU reveals further transformations via EU formation, transforming in turn into AO, as highlighted by the kinetic profiles of the two intermediates (Figure 6B). Similarly, the 1,1′-DEU structure **15** is transformed into AO, although at a slower rate and to a lesser extent. In addition, urea is formed after 1 h of irradiation.

Theoretical studies: To verify the reliability of the proposed degradation products, some theoretical calculation were performed. The aim was to achieve confirmation of the attack points of ·OH radicals and the position of the unpaired elec-

trons in the intermediate products of reaction by analysis of electron densities and net atomic charges. Additionally, an energetic profile for the formation of the five-membered ring was elaborated (see Scheme 3 for MU). It shows that the pathways leading to the formation of the key intermediate are characterized by favourable energetic profiles and that the initial formation of a carbon-centered radical, resulting from a C–H bond cleavage, is in agreement with literature data.[30]

The computation methods used were MOPAC, for calculating frontier electrons densities, and PM13, for calculating net atomic charges, both in gas phase and in water. The same calculations were performed by the B3LYP/6–31G ab initio method. The experimental results were unambiguously confirmed. The frontier electron densities and the point charges of all atoms for formamide, urea, and further compounds, calculated in water, are listed in Table 4. Looking closer at formamide and urea, the results of point charges reveals that the nitrogen atom(s) (having negative values) adsorbed more on the positive TiO_2 surface than the oxygen atom in the C=O moiety. With respect to formamide, the $^{\bullet}OH$ radical initially withdraws the proton of −CHO to generate CO_2 and NH_3. Considering alkyl derivatives, net atomic charges indicate that methyl groups are the preferential initial points of attack of $^{\bullet}OH$ radicals, while the nitrogen atoms are the main radical sites of subsequent degradation steps.

Conclusions

Both the methyl- and ethylurea derivatives have been shown to be easily degraded in the presence of titanium dioxide with similar kinetics, independent of the entity and the nature of the substitution. In contrast, the types of the formed intermediates and the rate and extension of the final mineralization are strongly dependent on the number of methyl or ethyl groups.

These observations have been rationalized within the framework of a transformation mechanism in which all the investigated molecules (and the recognized intermediate compounds) are involved. In all cases, N-demethylation represents only a secondary pathway, while the main transformation proceeds by means of the unexpected cyclization of MU, 1,1′- and 1,3-DMU, EU and 1,3′-DEU with the formation of (methyl)-amino-2,3-dihydro-1,2,4-oxadiazol-3-one as the major intermediate. Furthermore, the presence of an electron-donor group, such as a methyl or an ethyl group, favours the release of the nitrogen atom (oxidation state −3) in the form of nitrate (oxidation state +4) and the mineralization of carbon, with respect to the unsubstituted urea.

The understanding of the oxido/reductive reactions occurring for the alkylurea derivative may be useful in gaining information on naturally occurring transformations in which these moieties are involved.

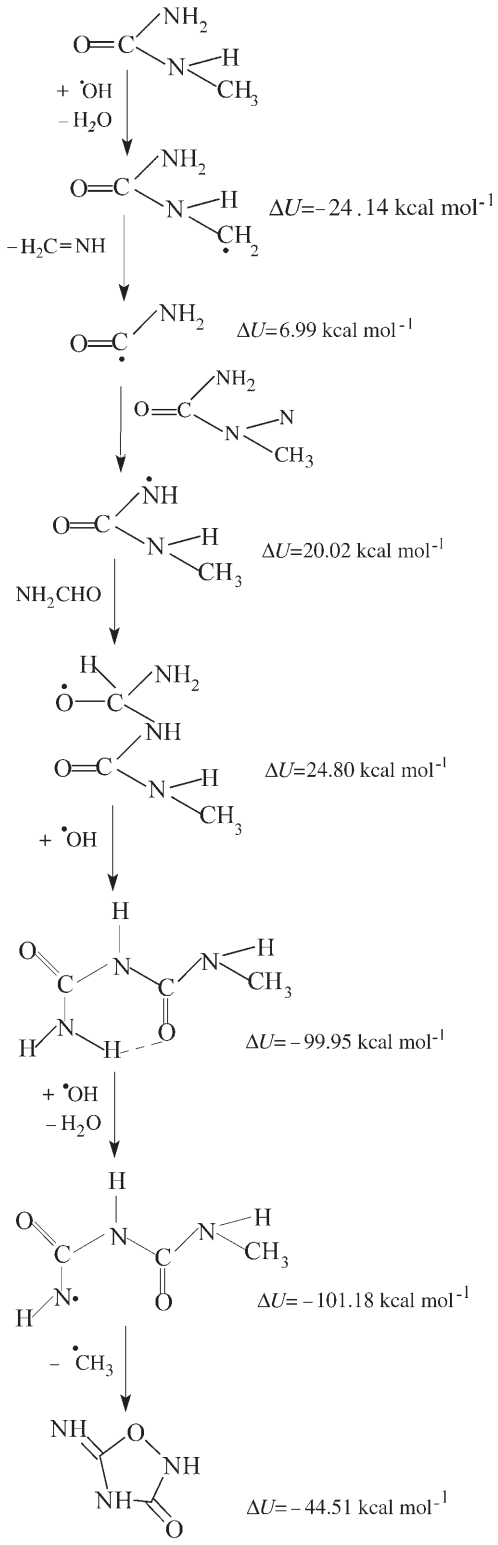

Scheme 3. Energetic profiles for the formation of AO from MU. The calculations have been done by using the B3LYP/6–31G theory.

Table 4. Calculated point charge and electron densities for urea, methylurea, dimethylureas, tetramethylurea and ethylureas in aqueous solution using the MOPAC/PM3 method.

Formamide

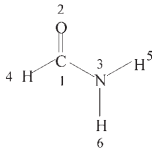

Atom no.	Type	Electron density	Point charge
1	C	3.797	0.203
2	O	6.793	−0.793
3	N	4.702	0.298
4	H	0.861	0.139
5	H	0.930	0.070
6	H	0.918	0.082

Urea

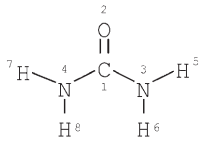

Atom no.	Type	Electron density	Point charge
1	C	3.828	0.172
2	O	6.807	−0.807
3	N	4.861	0.139
4	N	4.860	0.140
5	H	0.910	0.090
6	H	0.912	0.088
7	H	0.910	0.090
8	H	0.912	0.088

N-Methylurea

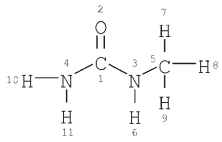

Atom no.	Type	Electron density	Point charge
1	C	3.734	0.266
2	O	6.682	−0.682
3	N	5.014	−0.014
4	N	4.943	0.057
5	C	4.095	−0.095
6	H	0.884	0.117
7	H	0.945	0.055
8	H	0.937	0.063
9	H	0.94	0.051
10	H	0.909	0.091
11	H	0.909	0.091

N,*N*-Dimethylurea

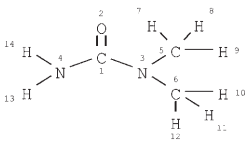

Atom no.	Type	Electron density	Point charge
1	C	3.719	0.281
2	O	6.667	−0.667
3	N	5.050	−0.050
4	N	4.944	0.056
5	C	4.094	−0.094
6	C	4.106	−0.105
7	H	0.936	0.064
8	H	0.932	0.068
9	H	0.946	0.055
10	H	0.942	0.058
11	H	0.934	0.066
12	H	0.925	0.075
13	H	0.904	0.096
14	H	0.903	0.097

1,3-Dimethylurea

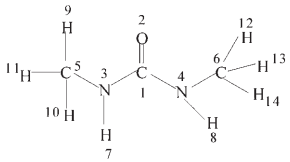

Atom no.	Type	Electron density	Point charge
1	C	4.711	0.289
2	O	6.643	−0.643
3	N	5.016	−0.016
4	N	5.015	−0.015
5	C	4.096	−0.096
6	C	4.096	−0.096
7	H	0.882	0.118
8	H	0.882	0.118
9	H	0.949	0.051
10	H	0.936	0.064
11	H	0.944	0.056
12	H	0.949	0.051
13	H	0.936	0.064
14	H	0.944	0.056

Tetramethylurea

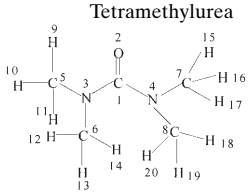

Atom no.	Type	Electron density	Point charge
1	C	3.684	0.316
2	O	6.617	-0.496
3	N	5.025	-0.025
4	N	5.043	−0.043
5	C	4.095	−0.095
6	C	4.116	−0.115
7	C	4.094	−0.094
8	C	4.117	−0.177
9	H	0.929	0.072
10	H	0.939	0.061
11	H	0.945	0.055
12	H	0.941	0.059
13	H	0.923	0.077
14	H	0.927	0.073
15	H	0.928	0.072
16	H	0.947	0.053
17	H	0.940	0.060
18	H	0.926	0.074
19	H	0.925	0.075
20	H	0.940	0.060

Ethylurea

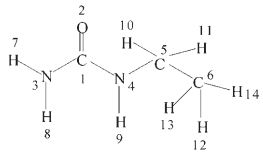

Atom no.	Type	Electron density	Point charge
1	C	3.684	0.270
2	O	6.617	−0.680
3	N	5.025	0.054
4	N	5.043	−0.023
5	C	4.095	−0.082
6	C	4.116	−0.126
7	H	0.994	0.091
8	H	0.917	0.09
9	H	0.929	0.118
10	H	0.939	0.068
11	H	0.945	0.065
12	H	0.941	0.051
13	H	0.923	0.049
14	H	0.927	0.054

Acknowledgements

We thank A. Deagostino and M. Clericuzio for NMR analysis, G. Magnacca for IR investigations, and C. Canepa for stimulating discussions. The work carried out in Tokyo was supported by the "Academic Frontier" Project for Private Universities from the Japanese Ministry of Education, Culture, Sports, Science and Technology (MEXT), as well as the Grant-in-Aid for Science Research (No. 10640569) of MEXT (H.H.).

[1] A. Aguera, E. Almansa, A. Tejedor, A. Fernandez-Alba, S. Malato, M. I. Maldonado, *Environ. Sci. Technol.* **2000**, *34*, 1563–1571.

[2] C. Bouquet-Somrani, F. Fajula, A. Finiels, P. Graffin, P. Geneste, J. L. Olive, *New J. Chem.* **2000**, *24*, 999–1002.

[3] K. M. Madyastha, G. R. Sridhar, *Biochem. Biophys. Res. Commun.* **1998**, *249*, 178–181.

[4] H. M. Neels, A. C. Sierens, K. Naelaerts, S. L. Scharpe, G. M. Hatfield, W. E. Lambert, *Clin. Chem. Lab. Med.* **2004**, *42*, 1228–1255.

[5] S. R. Nagarajan, A. G. De Crescenzo, D. P. Getman, H. F. Lu, J. A. Sikorski, J. L. Walker, J. J. McDonald, K. A. Houseman, G. P. Kocan, N. Kishore, P. P. Mehta, C. L. Funkes-Shippy, L. Blystone, *Bioorg. Med. Chem.* **2003**, *11*, 4769–4777.

[6] C. Jaussaud, O. Paisse, R. Faure, *J. Photochem. Photobiol. A* **2000**, *130*, 157–162.

[7] Praveenkumar, R. Brumme, *Fert. Res.* **1995**, *41*, 117–124.

[8] F. Wöhler, *Ann. Phys. Chem.* **1828**, *88*, 253–256.
[9] S. Kuwabata, H. Yamauchi, H. Yoneyama, *Langmuir* **1998**, *14*, 1899–1904.
[10] A. Fujiishima, K. Honda, *Nature* **1972**, *238*, 37–38.
[11] C. Minero, G. Mariella, V. Maurino, E. Pelizzetti, *Langmuir* **2000**, *16*, 2632–2641.
[12] M. A. Fox, M. T. Dulay, *Chem. Rev.* **1993**, *93*, 341–357.
[13] M. R. Hoffmann, S. T. Martin, W. Choi, D. W. Bahnemann, *Chem. Rev.* **1995**, *95*, 69–96.
[14] S. Y. Panshin, D. S. Carter, E. R. Bayless, *Environ. Sci. Technol.* **2000**, *34*, 2131–2137.
[15] P. Calza, C. Medana, C. Baiocchi, P. Branca, E. Pelizzetti, *J. Chromatogr. A* **2004**, *1049*, 115–125.
[16] P. Calza, E. Pelizzetti, M. Brussino, C. Baiocchi, *J. Am. Soc. Mass Spectrom.* **2001**, *12*, 1286–1295.
[17] P. Calza, C. Medana, M. Pazzi, C. Baiocchi, E. Pelizzetti, *J. Pharm. Biomed. Anal.* **2004**, *35*, 9–19.
[18] E. Pelizzetti, P. Calza, G. Mariella, V. Maurino, C. Minero, H. Hidaka, *Chem. Commun.* **2004**, *13*, 1504–1505.
[19] D. Y. Ra, N. S. Cho, S. K. Kang, E. S. Choi, H. H. Suh, *J. Chem. Soc. Perkin Trans. 1* **1999**, *2*, 81–83.
[20] T. Suyama, N. Ozawa, N. Suzuki, *Bull. Chem. Soc. Jpn.* **1994**, *67*, 307–308.
[21] Y. W. Ding, Y. Wu, C. Z. Fan, *Huaxue Wuli Xuebao* **2002**, *15*, 465–470.
[22] E. Pelizzetti, C. Minero, *Colloids Surf. A* **1999**, *151*, 321–327.
[23] P. Calza, E. Pelizzetti, C. Minero, *J. Appl. Electrochem.* **2005**, *35*, 665–673.
[24] G. K. C. Low, S. R. McEvoy, R. W. Matthews, *Environ. Sci. Technol.* **1991**, *25*, 460–467.
[25] K. Nohara, H. Hidaka, E. Pelizzetti, N. Serpone, *Catal. Lett.* **1996**, *36*, 115–118.
[26] P. Piccinini, C. Minero, M. Vincenti, E. Pelizzetti, *J. Chem. Soc. Faraday Trans.* **1997**, *93*, 1993–2000.
[27] C. Minero, P. Piccinini, P. Calza, E. Pelizzetti, *New J. Chem.* **1996**, *20*, 1159–1164.
[28] V. Maurino, C. Minero, E. Pelizzetti, P. Piccinini, N. Serpone, H. Hidaka, *J. Photochem. Photobiol. A* **1997**, *109*, 171–176.
[29] V. Augugliaro, J. Blanco Galvez, J. Caceres Vasquez, E. Garcia Lopez, V. Loddo, M. J. Lopez Muñoz, S. Malato Rodriguez, G. Marcì, L. Palmisano, M. Schiavello, J. Soria Ruiz, *Catal. Today* **1999**, *54*, 245–253.
[30] Y. S. Kang, H. J. D. McManus, L. Kevan, *Radiat. Phys. Chem.* **1994**, *44*, 323–327.

Received: March 15, 2005
Revised: July 7, 2005
Published online: October 10, 2005

